

Surface effects in frustrated magnetic materials: phase transition and spin resistivity

H T Diep (Iptm, ucp)

in collaboration with Yann Magnin, V. T. Ngo, K. Akabli

Plan:

- I. Introduction
- II. Surface spin-waves, surface magnetization:
Methods, Examples
- III. Surface phase transitions: Methods, Examples
- IV. Surface spin resistivity: Methods, Examples
- V. Conclusion

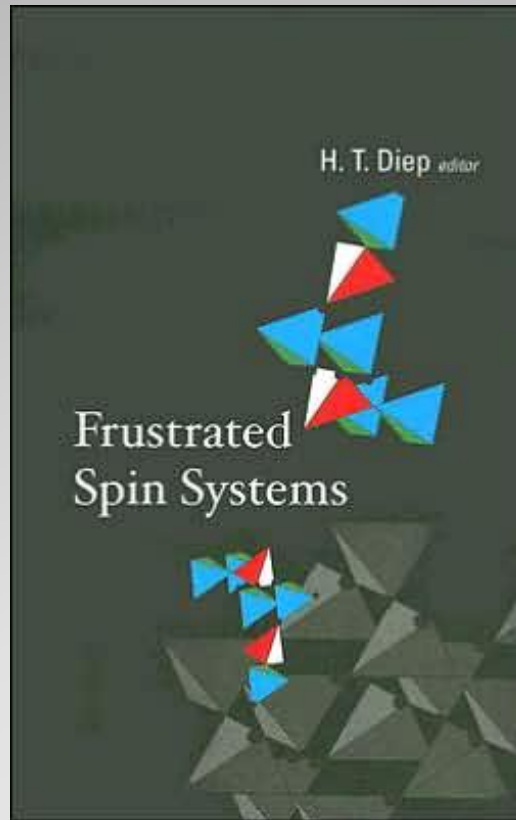
I. Introduction:

Physics at surfaces has been intensively developed over the past thirty years. Many spectacular properties due to the presence of surfaces have been discovered and used in industrial devices.

Surface effects in those small-scale systems give rise to quite different properties from bulk ones. In this talk, I just recall some fundamental properties for understanding surface magnetization, surface phase transition and surface spin transport in frustrated systems.

In the seventies, until the nineties, much efforts have been made to look for and to understand localized surface modes in magnon, phonon, plasmon ... spectra. In magnetic thin films, for example, we can show that low-lying acoustic surface spin-waves reduce the Curie temperature, can give magnetically dead surface layers, ... Optical surface spin-waves on the other hand enhance surface magnetization,

- In my works in general, I considered often situations near the borders of several phases of different symmetries in the ground state. The borders are due to competing interactions between spins.
- A family of such systems are called "**frustrated systems**". These systems are subject of investigations for more than 20 years (see reviews in "Frustrated Spin Systems").
- We have solved exactly (see reference next page) a number of models where one finds all interesting effects: high GS degeneracy, reentrance phenomenon, order by disorder, partial disorder, successive phase transition, disorder lines etc.



**See the chapter
« Exactly solved frustrated models »
by H T Diep and H. Giacomini, pp. 1-60
World Scientific 2005**

- Of course, surface magnetism bears these effects if necessary ingredients exist in thin films. I will show a few cases in this talk.

It has been shown a long time ago that low-lying-energy surface-localized modes play an important role in thermodynamic properties of thin films: low surface magnetization, reduction of T_c , (see Diep-The-Hung et al. Physica Status Solidi b, 93, 352 (1979))

Since the geometry of very small systems (dots, thin films, ...) and their surface conditions are complicated, analytical calculations are often impossible. One needs therefore NUMERICAL SIMULATIONS.

Some problems in my interest:

- Surface Elementary Excitations, Transition, Resistivity
- Adsorption: Pb on Cu, ...
- Effects of Surface Interaction Parameters; Surface spins, Surface Magnetic Moment, Surface Anisotropy : magnitude, sign, orientation, Surface Exchange Interaction

Our recent works

- Reorientation transition in films with dipolar interaction
- Effects of frustrated surfaces on non frustrated films
- Frustrated Films
- Criticality of ferromagnetic films: thickness effect
- Cross-over from first to second order of the transition in FCC AF films
- Surface spin resistivity in magnetically ordered materials

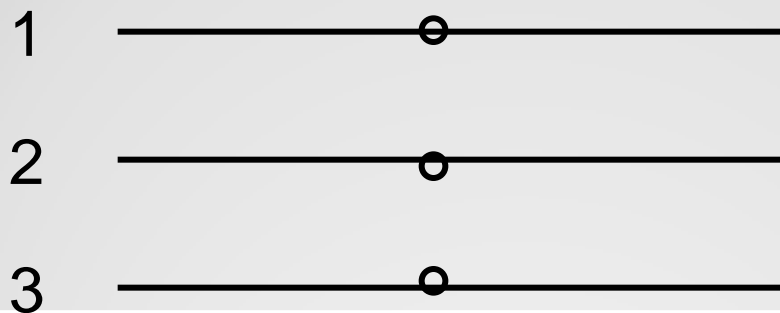
Methods: GF theory, MC simulations (histogram, multi-histogram, Wang-Landau flat histogram techniques)

III. Surface Spin-Waves (SW):

It is very simple to calculate the spin-wave spectrum for a semi-infinite crystal or a thin film, by using for instance,

- Equation of motion
- Spin-wave theory
- Green's function method

One obtains spin-wave spectrum with or without localized surface spin-wave modes (acoustic or optical)



Green's function method for surface magnetism

In the local framework:

$$\begin{aligned}\mathcal{H} = & - \sum_{\langle i,j \rangle} J_{i,j} \left\{ \frac{1}{4} (\cos \theta_{ij} - 1) (S_i^+ S_j^+ + S_i^- S_j^-) \right. \\ & + \frac{1}{4} (\cos \theta_{ij} + 1) (S_i^+ S_j^- + S_i^- S_j^+) \\ & + \frac{1}{2} \sin \theta_{ij} (S_i^+ + S_i^-) S_j^z - \frac{1}{2} \sin \theta_{ij} S_i^z (S_j^+ + S_j^-) \\ & \left. + \cos \theta_{ij} S_i^z S_j^z \right\} - \sum_{\langle i \rangle} I_i (S_i^z)^2\end{aligned}$$

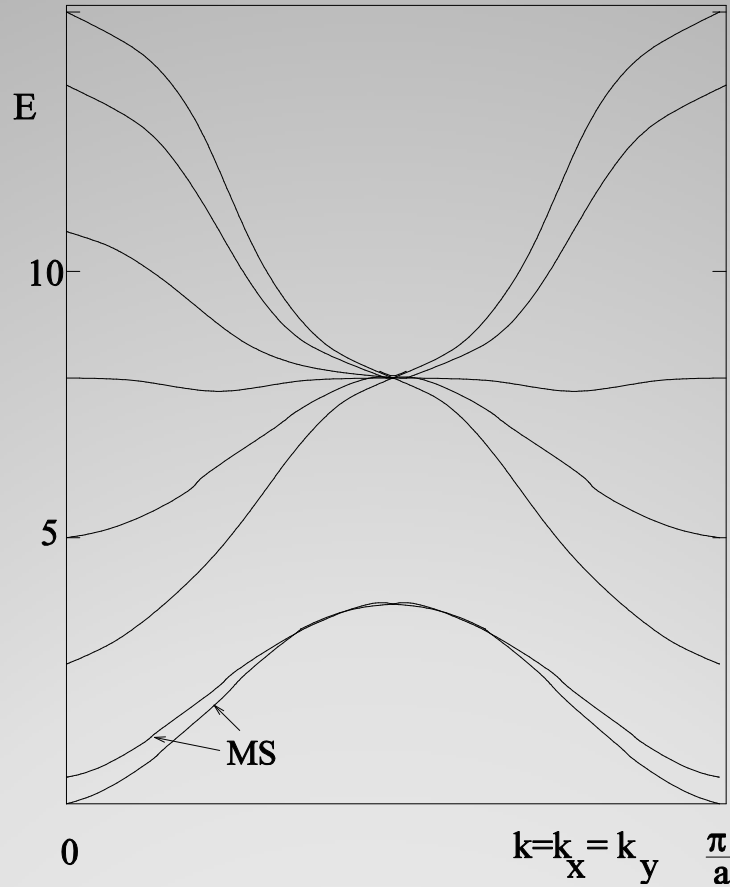
where $\cos(\theta_{ij})$ is the angle between two NN spins.

We define two double-time GF by?

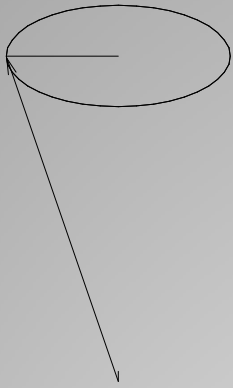
$$\begin{aligned}G_{ij}(t, t') &= \ll S_i^+(t); S_j^-(t') \gg, \\ F_{ij}(t, t') &= \ll S_i^-(t); S_j^-(t') \gg.\end{aligned}$$

$$\mathbf{g} = \begin{pmatrix} g_{1,n'} \\ f_{1,n'} \\ \vdots \\ g_{N_z,n'} \\ f_{N_z,n'} \end{pmatrix}, \mathbf{u} = \begin{pmatrix} 2 \langle S_1^z \rangle \delta_{1,n'} \\ 0 \\ \vdots \\ 2 \langle S_{N_z}^z \rangle \delta_{N_z,n'} \\ 0 \end{pmatrix},$$

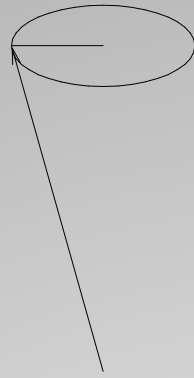
$$\mathbf{M}(\omega) = \begin{pmatrix} A_1^+ & B_1 & D_1^+ & D_1^- & \cdots \\ -B_1 & A_1^- & -D_1^- & -D_1^+ & \vdots \\ \vdots & \cdots & \cdots & \cdots & \vdots \\ \vdots & C_{N_z}^+ & C_{N_z}^- & A_{N_z}^+ & B_{N_z} \\ \cdots & -C_{N_z}^- & -C_{N_z}^+ & -B_{N_z} & A_{N_z}^- \end{pmatrix},$$



Spin-wave spectrum of a 8-layer ferromagnetic BCC film



$n = 1$



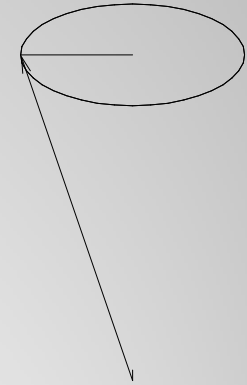
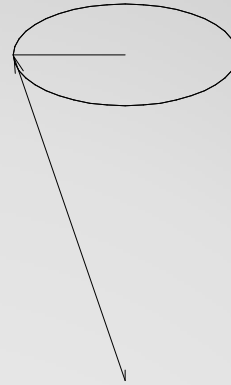
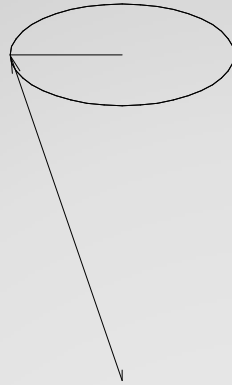
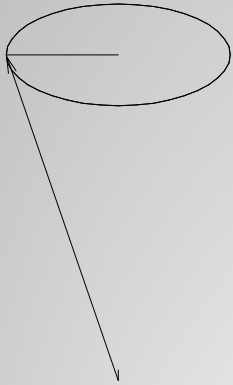
$n = 2$



$n = 3$



$n = 4$



Surface Spin-Wave Mode: damping from first layer inward

Surface Magnetization:

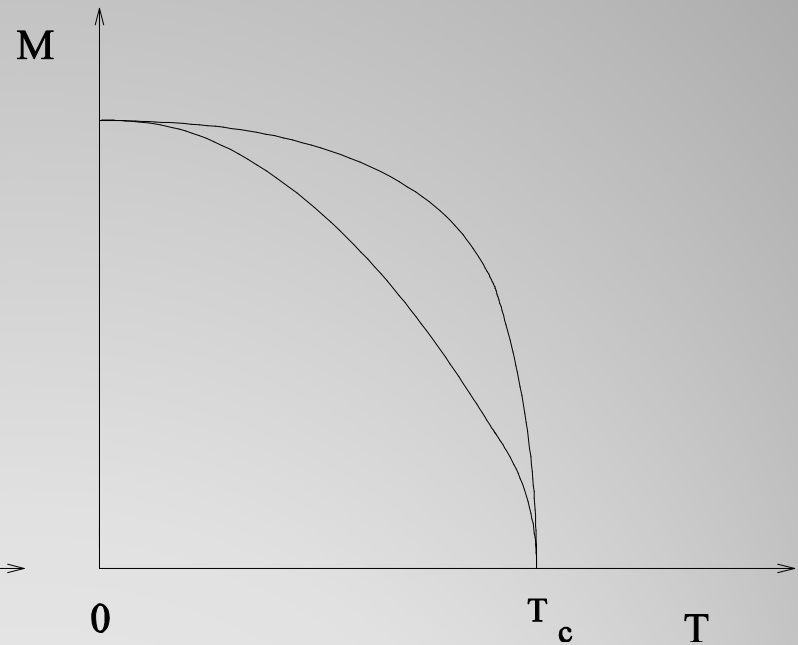
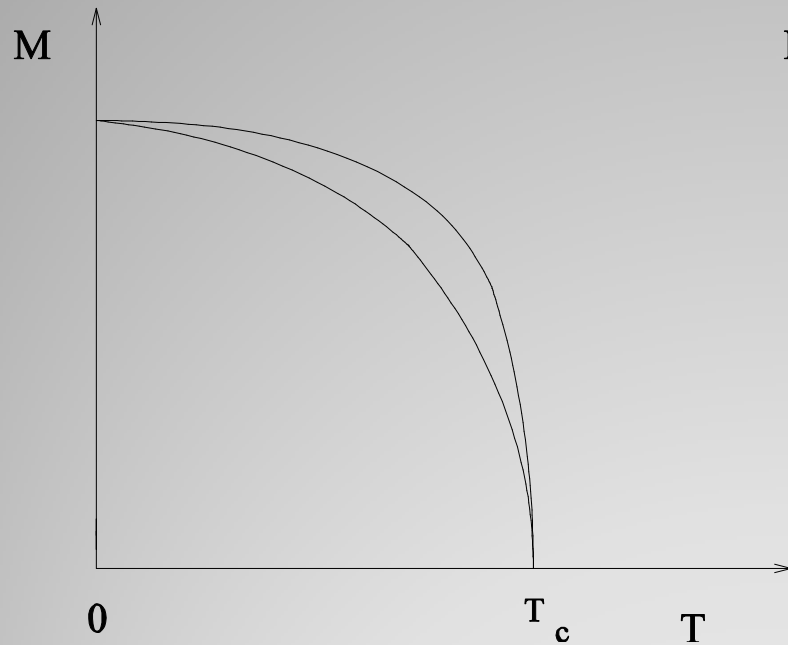
One can calculate the layer magnetization at a given T using the spin-wave spectrum obtained by the GF method.

Self-consistent solution should be searched for all M_i ($i=1,2,3, \dots$). In practice, one retains only a few different magnetizations $M_1 \neq M_2 \neq M_3 \neq M_4 = M_5 = \dots$ for simplicity

$$M = \frac{1}{N_T} \sum_{n=1}^{N_T} \langle S_n^z \rangle = \frac{1}{2} - \frac{1}{N_T} \frac{1}{\Delta} \int \int dk_x dk_y \sum_{n=1}^{N_T} \sum_{i=1}^{N_T} \frac{f_n(E_i)}{e^{\beta E_i} - 1}$$

$$M = \frac{1}{2} - \frac{1}{N_T} \frac{1}{\Delta} \int \int dk_x dk_y \sum_{i=1}^{N_T} \frac{2M}{e^{\beta E_i} - 1}$$

$$\left[\frac{J}{k_B T_c} \right]^{-1} = \frac{2}{\Delta} \int \int dk_x dk_y \frac{1}{N_T} \sum_{i=1}^{N_T} \frac{2M}{E_i}$$



Magnetization of the first (lower) and second (upper) layers.
Left: film with cubic lattice
Right: film with BCC lattice

III. Surface Phase Transitions:

Multiple histogram technique for finite-size scaling

The multiple histogram technique is known to reproduce with very high accuracy the critical exponents of second order phase transitions.

The overall probability distribution at temperature T obtained from n independent simulations, each with N_j configurations, is given by

$$P(E, T) = \frac{\sum_{i=1}^n H_i(E) \exp[E/k_B T]}{\sum_{j=1}^n N_j \exp[E/k_B T_j - f_j]}, \quad (2)$$

where

$$\exp[f_i] = \sum_E P(E, T_i). \quad (3)$$

The thermal average of a physical quantity A is then calculated by

$$\langle A(T) \rangle = \sum_E A P(E, T) / z(T), \quad (4)$$

in which

$$z(T) = \sum_E P(E, T). \quad (5)$$

Thermal averages of physical quantities are thus calculated as continuous functions of T , now the results should be valid over a much wider range of temperature than for any single histogram.

Wang-Landau Monte Carlo Method

- Recently, Wang and Landau proposed a Monte Carlo algorithm for classical statistical models. The algorithm uses a random walk in energy space in order to obtain an accurate estimate for the density of states $g(E)$. This method is based on the fact that a flat energy histogram $H(E)$ is produced if the probability for the transition to a state of energy E is proportional to $g(E)^{-1}$.
- At the beginning of the simulation, the density of states (DOS) is set equal to one for all energies, $g(E) = 1$. In general, if E and E' are the energies before and after a spin is flipped, the transition probability from E to E' is

$$p(E \rightarrow E') = \min [g(E)/g(E'), 1]. \quad (2)$$

- Each time an energy level E is visited, the DOS is modified by a modification factor $f > 0$ whether the spin flipped or not, i.e. $g(E) \rightarrow g(E)f$. In the beginning of the random walk the modification factor f can be as large as $e^1 \sim 2.7182818$. A histogram $H(E)$ records how often a state of energy E is visited. Each time the energy histogram satisfies a certain “**flatness**” criterion, f is reduced according to $f \rightarrow f^{1/2}$ and $H(E)$ is reset to zero for all energies. The reduction process of the modification factor f is repeated several times until a final value f_{final} which is close enough to one. The histogram is considered as flat if

$$H(E) \geq x\% \langle H(E) \rangle \quad (3)$$

for all energies, where the flatness parameter $0\% < x\% < 100\%$ controls the accuracy of the estimated $g(E)$, with increasing accuracy as $x\%$ approaches unity. $\langle H(E) \rangle$ is the average histogram. Thermodynamic quantities (Wang-Landau, Brown) can be evaluated using the canonical distribution at any temperature T by

$$P(E,T) = g(E) \exp(-E/k_B T) / Z$$

where Z is the partition function defined by

$$z = \sum g(E) \exp(-E/k_B T)$$

Frustrated surface on non frustrated Heisenberg film (PRB 75, 035412(2007))

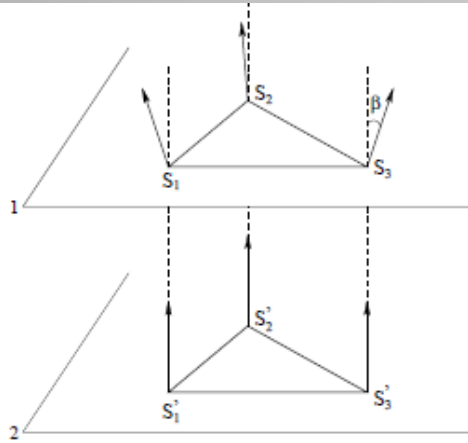


FIG. 1: Non collinear surface spin configuration. Angles between spins on layer 1 are all equal (noted α), while angles between vertical spins are β .

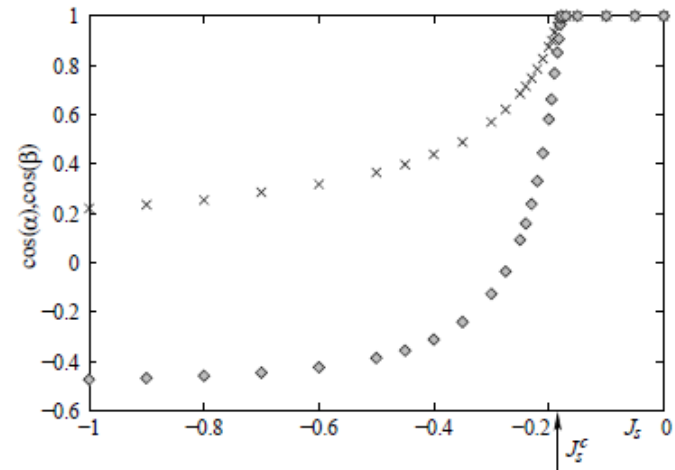


FIG. 2: $\cos(\alpha)$ (diamonds) and $\cos(\beta)$ (crosses) as functions of J_s . Critical value of J_s^c is shown by the arrow.

$$\frac{\partial H_p}{\partial \beta} = \left(\frac{27}{2} J_s + 9I_s \right) \cos \beta \sin \beta + \frac{3}{2} (J + I) \sin \beta = 0 \quad (5)$$

We have

$$\cos \beta = -\frac{J + I}{9J_s + 6I_s}. \quad (6)$$

$$G_{ij}(t, t') = \ll S_i^+(t); S_j^-(t') \gg,$$

$$F_{ij}(t, t') = \ll S_i^-(t); S_j^+(t') \gg.$$

$$\mathbf{M}(\omega) = \begin{pmatrix} A_1^+ & B_1 & D_1^+ & D_1^- & \dots \\ -B_1 & A_1^- & -D_1^- & -D_1^+ & \vdots \\ \vdots & \dots & \dots & \dots & \vdots \\ \vdots & C_{N_z}^+ & C_{N_z}^- & A_{N_z}^+ & B_{N_z} \\ \dots & -C_{N_z}^- & -C_{N_z}^+ & -B_{N_z} & A_{N_z}^- \end{pmatrix}, \quad (16)$$

where

$$\begin{aligned} A_n^\pm &= \omega \pm \left[\frac{1}{2} J_n \langle S_n^z \rangle (Z\gamma) (\cos \theta_n + 1) \right. \\ &- J_n \langle S_n^z \rangle Z \cos \theta_n - J_{n,n+1} \langle S_{n+1}^z \rangle \cos \theta_{n,n+1} \\ &- J_{n,n-1} \langle S_{n-1}^z \rangle \cos \theta_{n,n-1} - Z I_n \langle S_n^z \rangle \\ &\left. - I_{n,n+1} \langle S_{n+1}^z \rangle - I_{n,n-1} \langle S_{n-1}^z \rangle \right], \end{aligned} \quad (17)$$

$$B_n = \frac{1}{2} J_n \langle S_n^z \rangle (\cos \theta_n - 1) (Z\gamma), \quad (18)$$

$$C_n^\pm = \frac{1}{2} J_{n,n-1} \langle S_n^z \rangle (\cos \theta_{n,n-1} \pm 1), \quad (19)$$

$$D_n^\pm = \frac{1}{2} J_{n,n+1} \langle S_n^z \rangle (\cos \theta_{n,n+1} \pm 1), \quad (20)$$

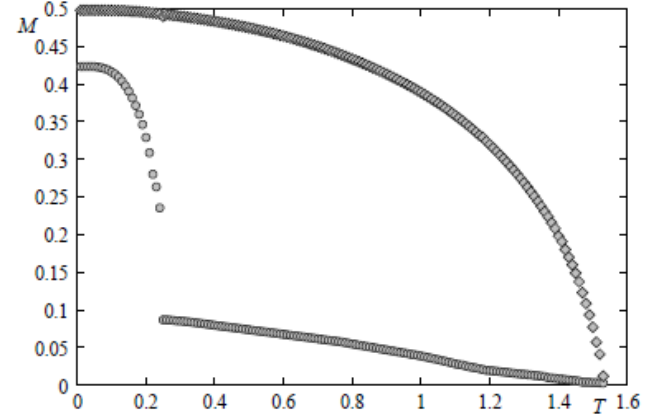


FIG. 3: First two layer-magnetizations obtained by the Green function technique vs. T for $J_s = -0.5$ with $I = -I_s = 0.1$. The surface-layer magnetization (lower curve) is much smaller than the second-layer one. See text for comments.

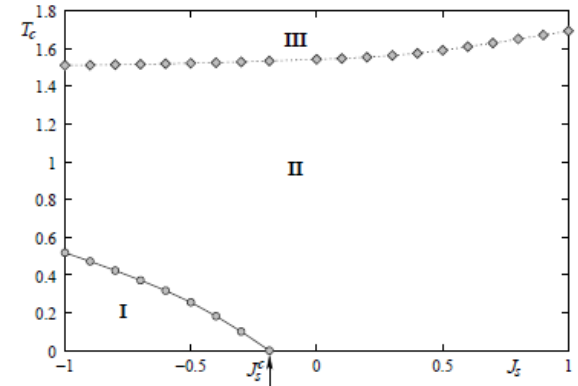


FIG. 5: Phase diagram in the space (J_s, T) for the quantum Heisenberg model with $N_z = 4$, $I = |I_s| = 0.1$. See text for the description of phases I to III.

Monte Carlo Results

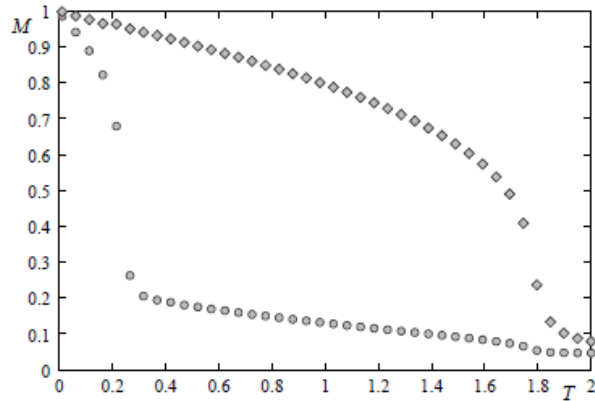


FIG. 7: Magnetizations of layer 1 (circles) and layer 2 (diamonds) versus temperature T in unit of J/k_B for $J_s = -0.5$ with $I = -I_s = 0.1$, $L = 36$.

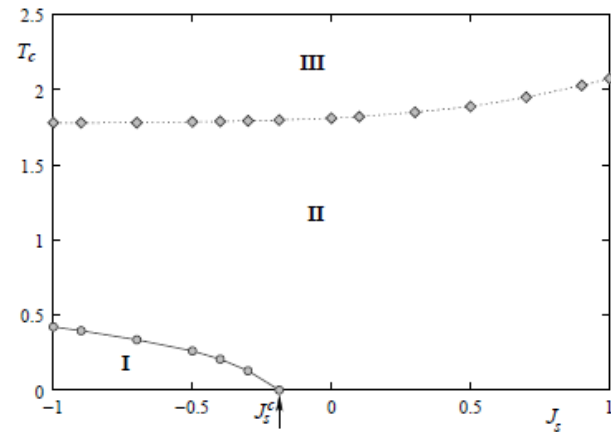


FIG. 10: Phase diagram in the space (J_s, T) for the classical Heisenberg model with $N_z = 4$, $I = |I_s| = 0.1$. Phases I to III have the same meanings as those in Fig. 5.

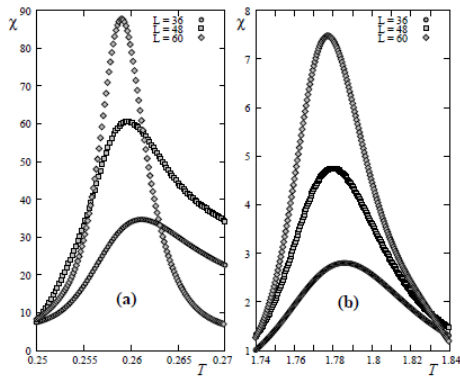


FIG. 13: Layer susceptibilities versus T for $L = 36, 48, 60$ with $J_s = -0.5$ and $I = -I_s = 0.1$. Left (right) figure corresponds to the first (second) layer susceptibility.

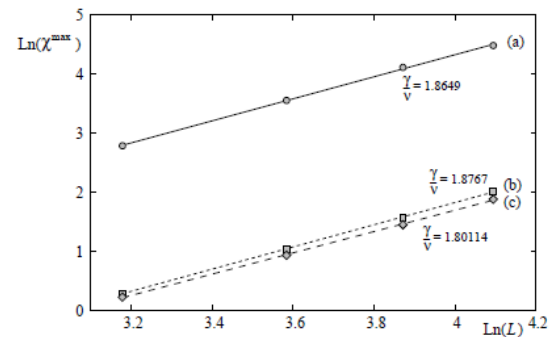


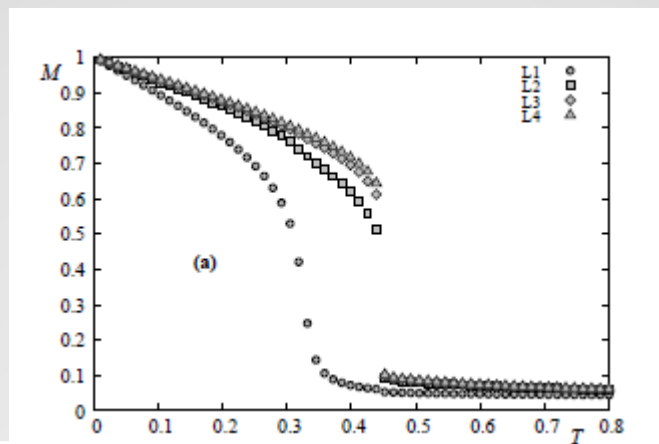
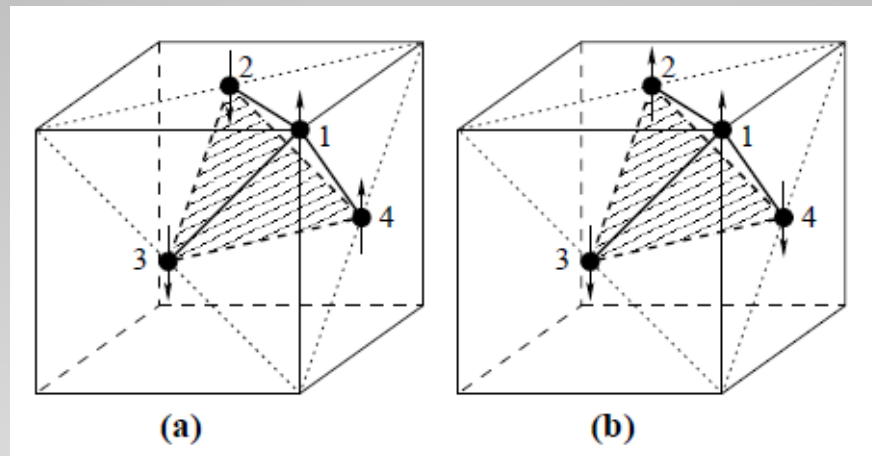
FIG. 16: Maximum of surface-layer susceptibility versus L for $L = 24, 36, 48, 60$ with $J_s = -0.5$ (a,b), $J_s = 0.5$ (c) and $I = |I_s| = 0.1$, in the $\ln - \ln$ scale. The slope gives γ/ν indicated in the figure for each case. See text for comments.

FRUSTRATED AF FCC HEISENBERG THIN FILMS (Phys.: Cond. Mat. 19, 386202 (2007))

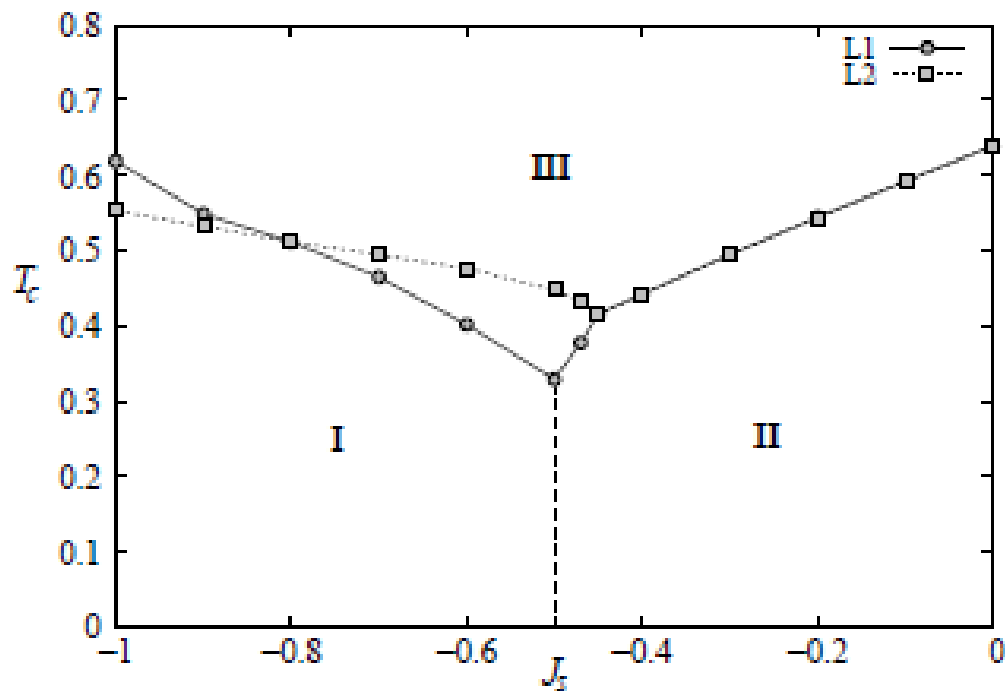
- Fully frustrated with infinite GS degeneracy
- Bulk; first-order transition
- Surface transition: ???

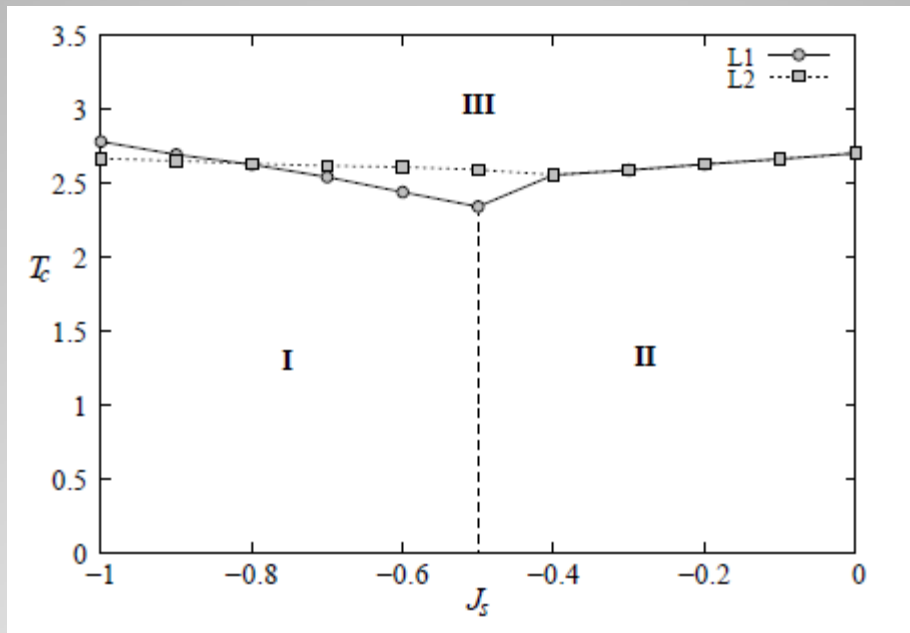
- MODEL: NN interaction with Ising-like uniaxial anisotropy

UPPER: GS for $J_s > -0.5 J$ (right), $J_s < -0.5 J$ (left)
LOWER: Layer magnetization for $J_s = -0.5 J$



Monte Carlo Phase Diagram in the space (T_c, J_s) . Discontinued line is first-order ($N_z=4$)





GF Phase Diagram

IV. SPIN RESISTIVITY

- **Resistivity in crystals: from phonons, impurities (charges, vacancies, defects, magnetic impurities, ...), magnetic ordering (spin-waves, ...), ...**

$$\rho(T) = \rho_0 + aT^2 + bT^5 + c \ln \frac{\mu}{T} + \rho_m$$

- **Phonon resistivity: T^5 at low T , linear in T at high T**
- **Spin resistivity, since the 50's: spin-wave scattering gives T^2 at low T (by spin-wave theory, mean-field theory) (cf. Turov 1955, Kasuya 1956). Scattering in a Fermi liquid gives also T^2**
- **Role of spin-spin correlation in spin resistivity: de Gennes-Friedel (1958), Langer-Fisher (1967), Haas (1967), ...**

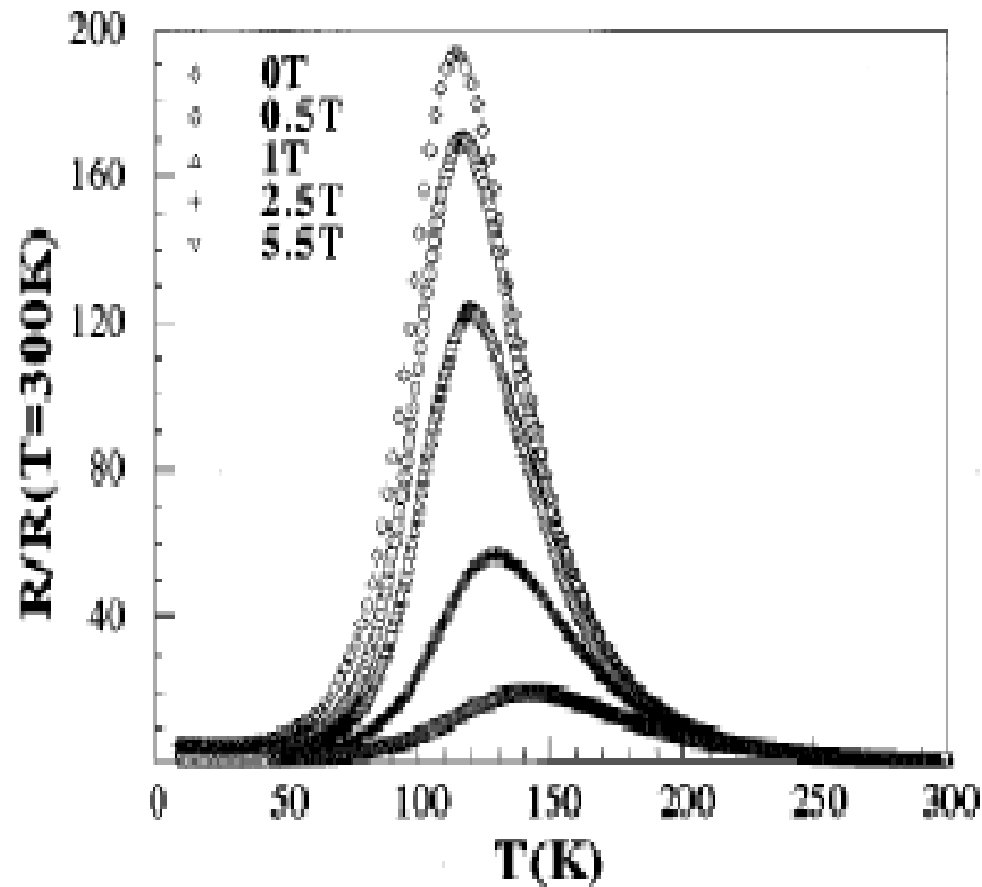


FIG. 2.5: Variation relative de la résistance entre 0 et 5.5 T en fonction de la température pour $(La_{1-x}Y_x)_{2/3}Ca_{1/3}MnO_3$ avec $x = 0.15$. (extraite de l'article de Martinez et al.[65]).

McGuire et al. PRB78(2008), LaFeAsO Tetra-Ortho Struct. Transition $T_c = 160$ K, SDW $T < T_c$ (AF order)

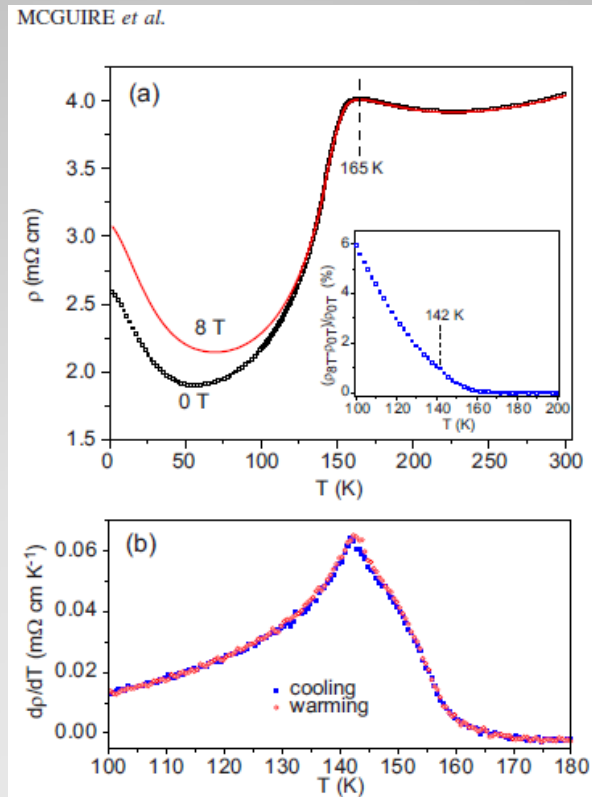


FIG. 6. (Color online) Effects of the phase transitions on the electrical transport of LaFeAsO. (a) The temperature dependence of the electrical resistivity with no applied magnetic field and with an applied field of 8 T. The inset in (a) shows the magnetoresistance calculated from the resistivity data. (b) The temperature derivative of the measured resistivity on cooling and warming illustrating the absence of thermal hysteresis. The effect of the structural transition at 160 K is shown. The peak in $d\rho/dT$ is near the magnetic transition temperature at 143 K.

X. H. Wang et al. PRL (2009), superconducting BaFe₂As₂

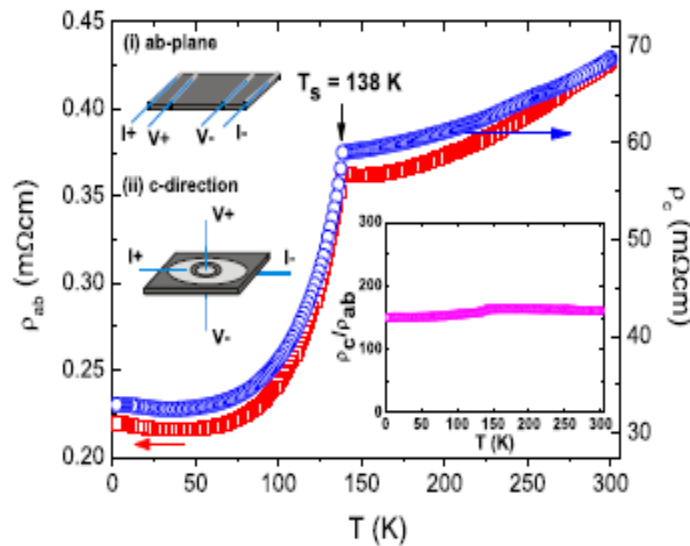


FIG. 2 (color online). Temperature dependence of in-plane and out-of-plane resistivity [$\rho_{ab}(T)$ (squares) and $\rho_c(T)$ (circles)] for single crystal BaFe₂As₂. The inset shows that the resistivity anisotropy (ρ_c/ρ_{ab}). ρ_c/ρ_{ab} is independent of temperature, indicating that transport in the ab plane and along the c -axis direction share the same scattering mechanism.

PRL 102, 117005 (2009) PHYSICAL REVIEW LETTERS

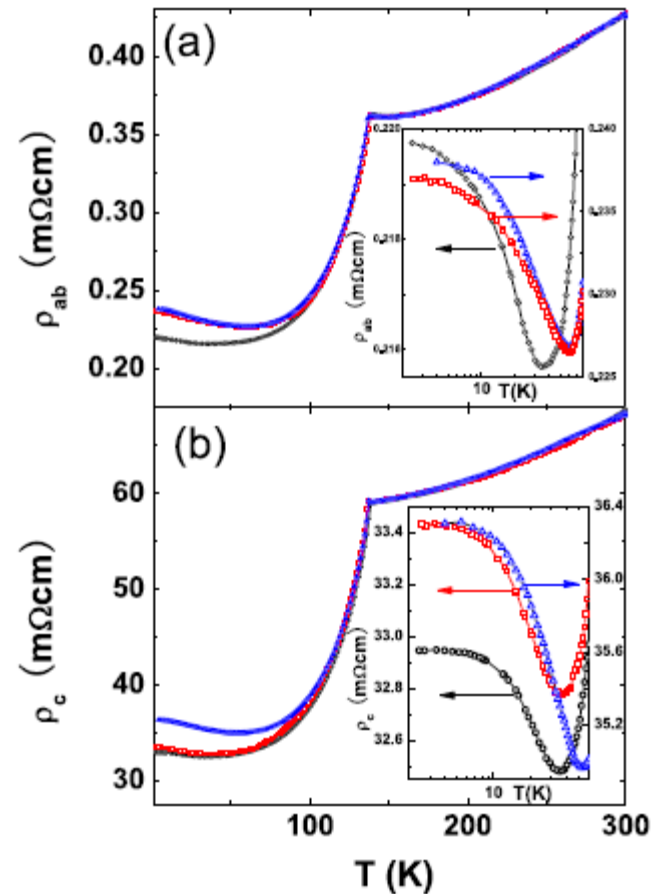


FIG. 4 (color online). Temperature dependence of in-plane and out-of-plane resistivity under magnetic field (H) of 0 and 6.5 T with $H \parallel$ to the ab plane and along the c axis, respectively. Zero-field resistivity (circles); $H \parallel ab$ plane (squares); and $H \parallel c$ -axis direction (triangles). Insets show the plot of low temperature ρ_{ab} and ρ_c vs T in log scale.

- **Our motivation:**
 - **Abundance of recent experiments on spin resistivity**
 - **Existing theories involving too many approximations (parabolic band, relaxation-time approximation, ...)**
 - **Absence of Monte Carlo (MC) simulations in this subject**
 - **Monte Carlo simulations can study complicated systems where theories cannot**
- **Our purpose:**
 - **Investigation of the effect of the magnetic ordering and the phase transition on the spin resistivity by MC simulations**
- **Our model:**
 - **Classical spin models with most important interactions**

Monte Carlo Simulation Method

- Lattice sample: thin film of dimension $N_x \times N_y \times N_z$
- Classical spins (Ising, XY, Heisenberg)
- Choice of Hamiltonian and parameters:
- Periodic boundary conditions in xy, reflecting condition in z
- Equilibrating the lattice spins before injecting itinerant spins, at a given T
- Itinerant spins travelling across the lattice, with different interactions
- Averaging physical quantities after stationary regime is reached
- Multi-step averaging procedure
- Resistivity

$$\rho = m/ne^2\tau$$

EFFECT OF MAGNETIC FIELD (FCC FERROMAGNET)

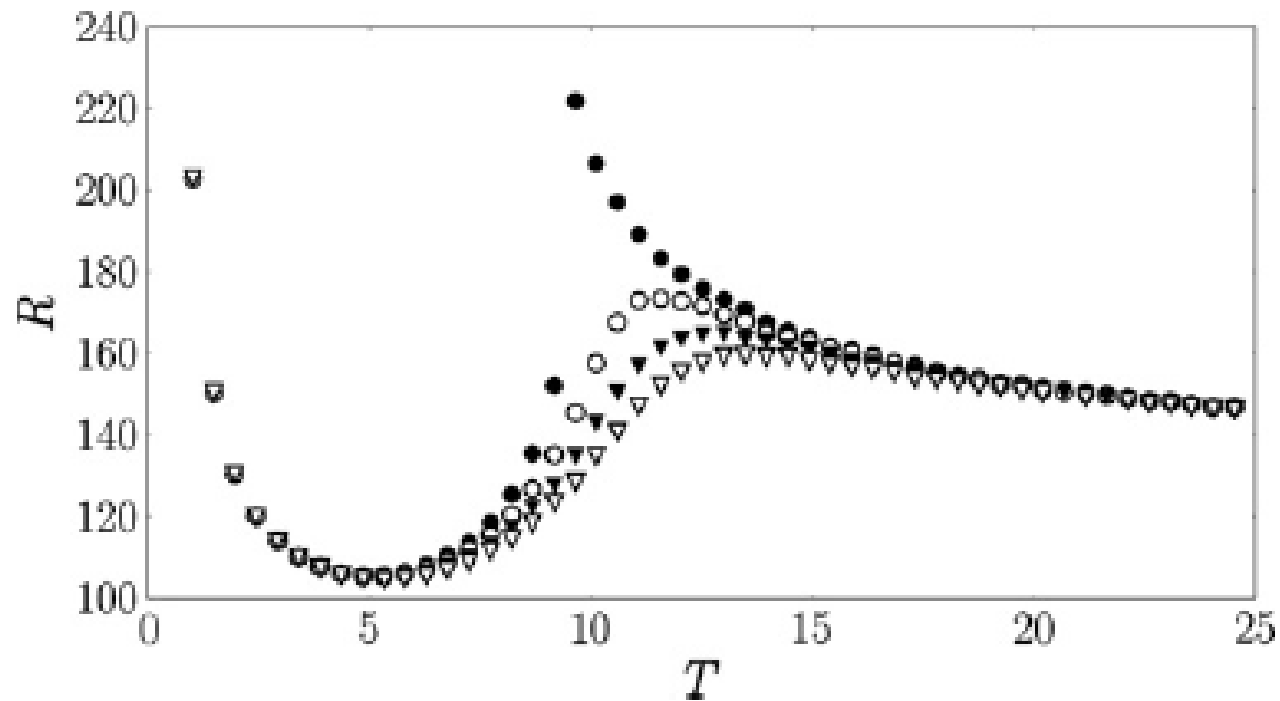
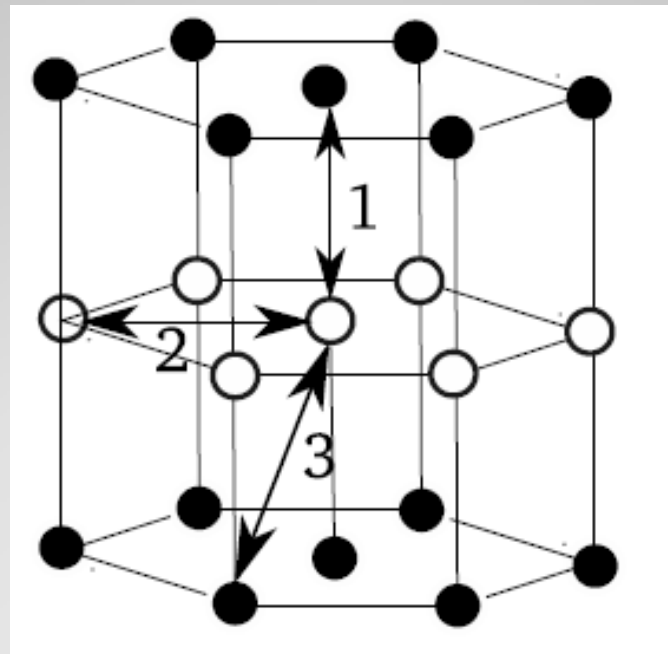


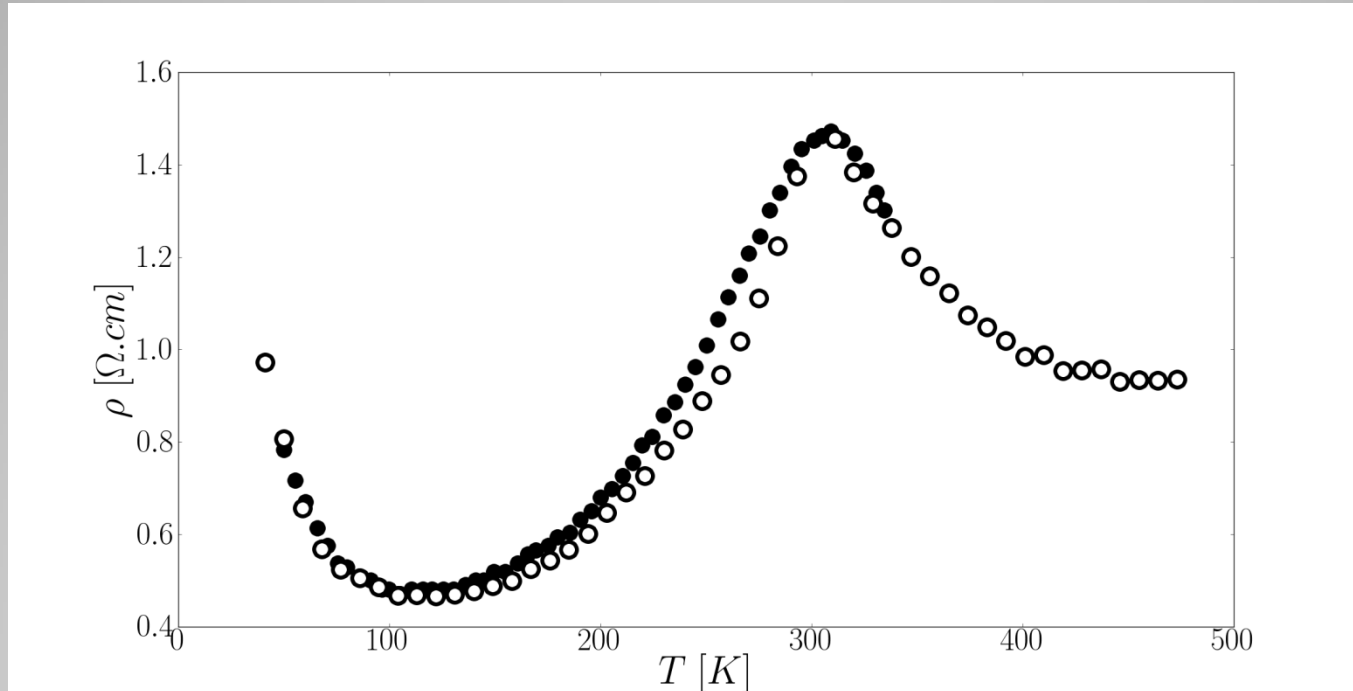
Fig. 4. Resistivity R in arbitrary unit versus temperature T , for different magnetic fields B : 0 (black circles), 0.25 (void circles), 0.5 (black triangles), 0.75 (void triangles). $I_0 = 2$ and other parameters taken the same as in Fig. 2.

W. Szuszkiewicz, E. Dynowska, B. Witkowska and B. Hennion: Phys. Rev. B **73** (2006) 104403.



Hexagonal NiAs-type MnTe: magnetic interactions

$J_1 = -21.5$ K, $J_2 = 2.55$ K, $J_3 = -9$ K, $I_0 = 2$ K, $S = 5/2$
Monte Carlo Results: $\tau = 0.1$ ps, $l = 1$ nm, $T_c = 310$ K
Black Circles: Experiment
Void Circles: Monte Carlo Results



X. He†, Y.Q. Zhang and Z.D. Zhang

J. Mater. Sci. Technol., 2011, 27(1), 64-68.

Surface Effect

- FCC AF FILM

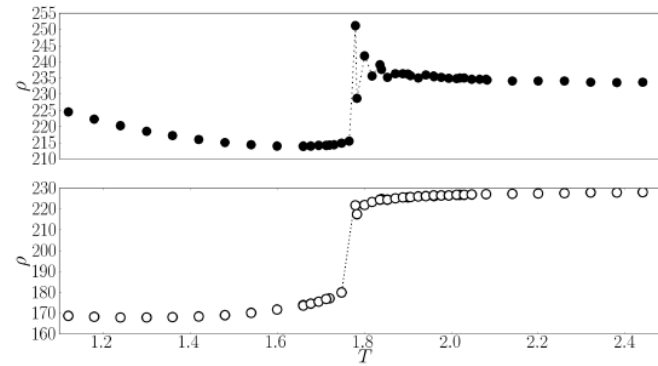


FIG. 5: Resistivity of thin film of size $N_x = N_y = 20$ and $N_z = 8$ for $N_0 = 1600$ itinerant spins versus T for $D_1 = a$ (black circles) and $D_1 = 1.25a$ (white circles), a being the lattice constant. Case of the first degenerate state. $J_s = J = -1.0$, $I_0 = K_0 = 0.5$, $D = 0.35$.

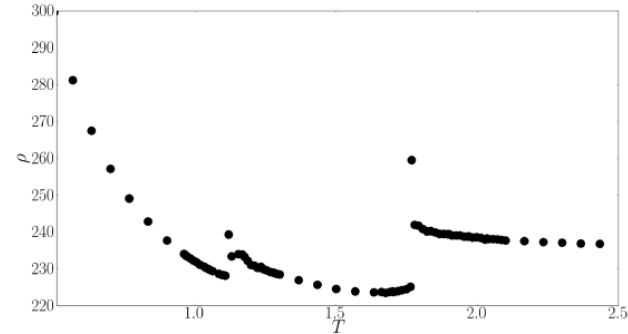
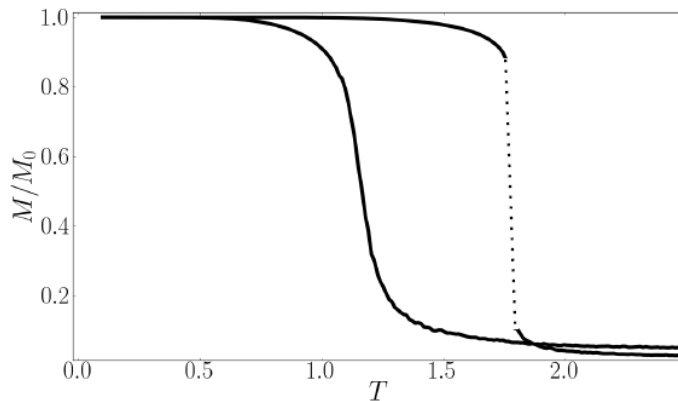
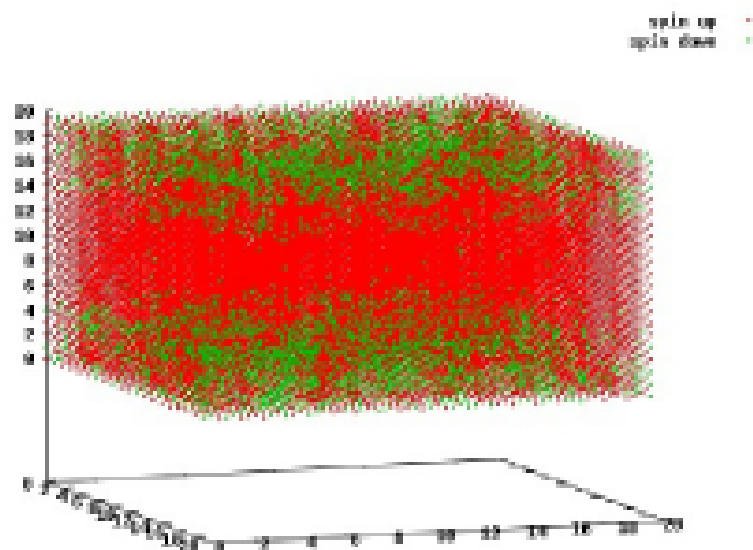


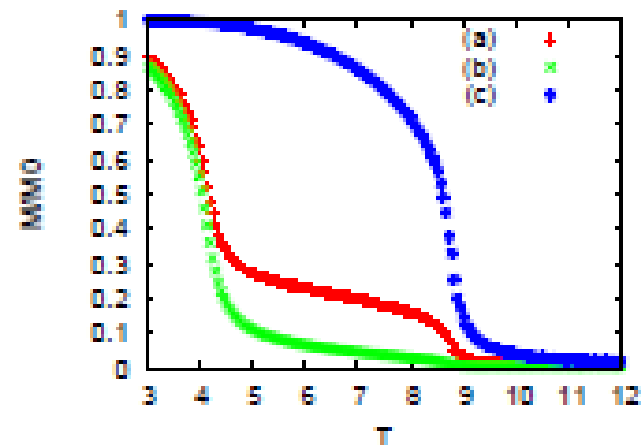
FIG. 11: Resistivity versus temperature T in the case shown in Fig. 10. There are two anomalies occurring respectively at the surface transition temperature and at the bulk one.

Effect of surfaces

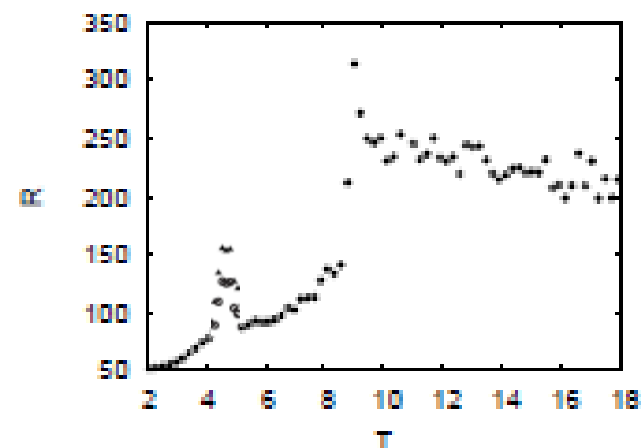


Artificial magnetic structure at $T_{c1} < T < T_{c2}$.

$J_s = 0.2 * J$, $T_{c1} = 4.20$ and $T_{c2} = 9.60$



M/M_0 versus T , blue : central layer, green : surface layer, red : whole system



V. Conclusion

- **Monte Carlo simulation is a very good tool: easy tuning of parameters for comparison with experiments.**

Recent works on spin resistivity:

- Temperature Dependence of Spin Resistivity in Ferromagnetic Thin Films, Phys. Rev. B **77**, 165433 (2008)
- Monte Carlo Study of the Spin Transport in Magnetic Materials, Computational Materials Science **49**, S204–S209 (2010).
- Theory and Simulation of Spin Transport in Antiferromagnetic Semiconductors: Application to MnTe, Phys. Rev. B (2011).
- Spin Resistivity in Frustrated Antiferromagnets, Phys. Rev. B **83** (2011)
- Spin Resistivity in the Frustrated J_1 - J_2 Model, Mod. Phys. L. B (2011)
- Spin Transport in Magnetically Ordered Systems: Effect of the Lattice Relaxation Time, Modern Phys. Letters B (2011).
- Monte Carlo Simulation of Spin Resistivity in Semiconducting MnTe, PRB (2012)